THE JOURNAL OF PHYSICAL CHEMISTRY Letters

Letter

pubs.acs.org/JPCL

# Nucleation of Graphene Layers on Magnetic Oxides: $Co_3O_4(111)$ and $Cr_2O_3(0001)$ from Theory and Experiment

John Beatty,[†,∥] Tao Cheng,[‡,∥] Yuan Cao,[†] M. Sky Driver,[†] William A. Goddard, III,[*,‡] and Jeffry A. Kelber[*,†]

[†]Department of Chemistry, University of North Texas, 1155 Union Circle, #305070, Denton, Texas 76203-5017, United States

[‡]Materials and Process Simulation Center, Department of Chemistry, California Institute of Technology, Pasadena, California 91125, United States

Supporting Information

**ABSTRACT:** We report directly grown strongly adherent graphene on $Co_3O_4(111)$ by carbon molecular beam epitaxy (C MBE) at 850 K and density functional theory (DFT) findings that the first graphene layer is reconstructed to fit the $Co_3O_4$ surface, while subsequent layers retain normal graphene structure. This adherence to the $Co_3O_4$ structure results from partial bonding of half the carbons to top oxygens of the substrate. This structure is validated by X-ray photoelectron spectroscopy and low-energy electron diffraction studies, showing layer-by-layer graphene growth with ∼0.08 electrons/carbon atom transferred to the oxide from the first graphene layer, in agreement with DFT. In contrast, for $Cr_2O_3$ DFT finds no strong bonding to the surface and C MBE on $Cr_2O_3(0001)$ yields only graphite formation at 700 K, with C desorption above 800 K. Thus strong graphene-to-oxide charge transfer aids nucleation of graphene on incommensurate oxide substrates and may have implications for spintronics.

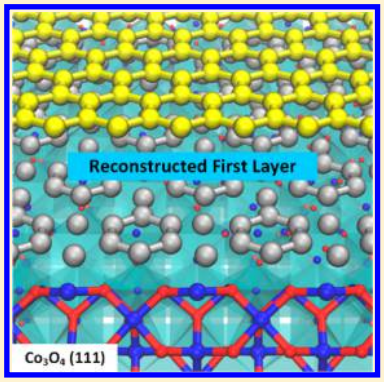


The long spin-diffusion length and high mobility of graphene make it attractive for emerging spintronics applications,[1,2] but the relative inefficiency of spin injection is a significant drawback.[3] Thus it is of considerable interest to use a magnetic insulator substrate or overlayer to induce spin polarization in graphene by interfacial spin interactions.[4−7] This would make industrially practical and scalable methods of growing graphene directly on such magnetic insulators of great technological and scientific significance. Recently, we used carbone molecular beam epitaxy (C MBE) on $Co_3O_4(111)$ to demonstrate[8,9] several layers of azimuthally oriented graphene. For spintronic device applications, growing similar films on $Cr_2O_3(0001)$ would offer several important advantages compared with other oxides because of its magnetoelectric properties[5,10] and the ability to produce a single magnetic domain via field cooling.[11] However, we find that C MBE on chromia yields only disordered graphite below ∼800 K and the desorption of C above this temperature. We use experiment and DFT to understand the origin of this dramatic difference between growth of graphene on $Co_3O_4(111)$ compared with $Cr_2O_3(0001)$ to provide insight into developing guidelines for obtaining cohesive graphene/oxide films.

Both oxides have similar in-plane O−O distances ∼2.86 Å,[12,13] which are significantly larger than that of graphene, suggesting the need for some covalent bonding to stabilize the first layer of graphene. Because any covalent bonding between C and O would transfer charge to the more electronegative partner, the O, we speculated that a strongly bound graphene on an oxide should transfer charge from the graphene to the oxide. This could account for the dramatic difference between these oxides because $Co_3O_4(111)$ is p-type, which should be favorable for charge transfer to the oxide and hence for covalent bonding to the first layer of C, whereas $Cr_2O_3(0001)$ is n-type under ultra-high vacuum (UHV) conditions,[14] which might be unfavorable. Thus we speculated that interfacial charge transfer between graphene and the oxide might play an important role in the quality of the graphene overlayer.

Studies of C MBE on $Co_3O_4(111)$ were carried out in a system equipped for X-ray photoelectron spectroscopy (XPS), low-energy electron diffraction (LEED), and MBE that has been previously described.[15] For studies on $Co_3O_4(111)$, Co(0001) films ∼25 to 30 Å thick were deposited directly on commercially available 1 cm × 1 cm $Al_2O_3(0001)$ substrates by MBE at 700 K, as previously described.[8] Film structure, thickness, and cleanliness were analyzed by XPS and LEED. XPS spectra were acquired in constant pass energy mode (22 eV) using unmonochromatized MgK$\alpha$ radiation. $Co_3O_4$ films 10 Å thick were prepared by direct oxidation of Co(0001) ($5 \times 10^{-7}$ Torr $O_2$, 650 K for 40 min), followed by annealing in UHV to ∼1000 K.

Studies of C deposition on $Cr_2O_3(0001)$/Co(0001) were carried out in a system previously described,[8] equipped for Auger electron spectroscopy (AES) using a cylindrical mirror analyzer and coaxial electron gun, reverse-view LEED, and the same electron beam evaporation source. AES data were

**Received:** October 8, 2016
**Accepted:** December 14, 2016
**Published:** December 14, 2016

ACS Publications © 2016 American Chemical Society



DOI: 10.1021/acs.jpclett.6b02325
J. Phys. Chem. Lett. 2017, 8, 188−192

acquired at 3000 eV primary beam energy and collected in the integral mode [N(E) vs E], then differentiated using the commercially available software. For studies on $Cr_2O_3$, ~1000 Å thick Co(0001) films were prepared by sputter deposition in a separate chamber, followed by sample transfer in ambient and annealing in $O_2$ and $H_2$ to remove C and O. $Cr_2O_3$ films were prepared by evaporative deposition of Cr on Co(0001) in ~$1 \times 10^{-6}$ Torr $O_2$ at room temperature, followed by an anneal in $1 \times 10^{-7}$ Torr $O_2$ at 800 K, with film structure and cleanliness verified by LEED and AES.

Indeed, our DFT calculations of graphene on $Co_3O_4$(111) find partial covalent bonding for the first graphene layer with a transfer of 0.083 electrons/carbon atom on average from the graphene, which is consistent with our experiments. In contrast, DFT calculations on graphene/$Cr_2O_3$(0001) find very little binding with no charge transfer,[6] which is consistent with our observation that C MBE on chromia yields only disordered graphite below ~800 K with desorption of C above this temperature. There is no experimental evidence of C to chromia charge transfer, in agreement with previous DFT calculations, indicating oxide-to-graphene charge transfer.[6]

These results suggest strongly that interfacial charge transfer from C to the oxide correlates with graphene nucleation. Hence the surface electronegativity or charge character of the oxide might serve as a useful design feature in selecting the oxide and its surface for the graphene/oxide film

To analyze the graphene oxide interface we carried out DFT calculations using the generalized gradient-corrected Perdew–Burke–Ernzerhof (PBE) functional including the D3BJ empirical correction to include London dispersion (vdW attraction). To obtain the correct band gap for the bulk phase calculation, we applied on-site Coulomb repulsion Hubbard U terms. The values of the U terms are taken from the work of Chen et al., which has been shown to provide a quite satisfactory description of the electronic structure of bulk $Co_3O_4$ with $U$ = 4.4 eV applied to the $Co^{2+}$ state and $U$ = 6.7 eV applied to the $Co^{3+}$state.[16] For surface calculations, a single $U$ value (−5.9 eV, a weighted average of the two $U$ values) is used for all Co ions due to difficulty in identifying the oxidation states of the surface Co ions and the inconsistency in calculating surface energy. This single $U$ value has been validated to reproduce the surface energy and relative stabilities of polar $Co_3O_4$(110) surface.[17] We used ultrasoft pseudopotentials to describe the O 2s, 2p and Co 3d, 4s valence electrons. We employed plane-wave energy cutoffs of 500 eV to ensure good convergence of the properties. All calculations were performed within the plane-wave pseudopotential scheme, as implemented in the Vienna ab initio simulation package (VASP) 5.3.1. Spin polarization was always included to describe exchange and correlation.

Calculations of bulk $Co_3O_4$ were performed using the 14-atom primitive unit cell of the spinel *Fd*-3*m* structure. We used a $6 \times 6 \times 6$ k-point grid to obtain a well-converged sampling of the Brillouin zone.

Surfaces were modeled using a periodic slab geometry, with consecutive slabs separated by a vacuum layer 15 Å wide. To study the properties of a single A or B termination, we considered symmetric slabs with odd numbers of layers so that the total dipole moment was zero. Although nonstoichiometric, these models provide useful information in the thick sample limit, when the effect of nonstoichiometry becomes negligible.[18] Structural optimizations were carried out by relaxing all atomic positions until all forces were $<1 \times 10^{-2}$ eV/A.

Figure 1 a shows the crystal structure of $Co_3O_4$ (*Fd*-3*m*). This spinel structure contains one $Co^{2+}$ and two $Co^{3+}$ per

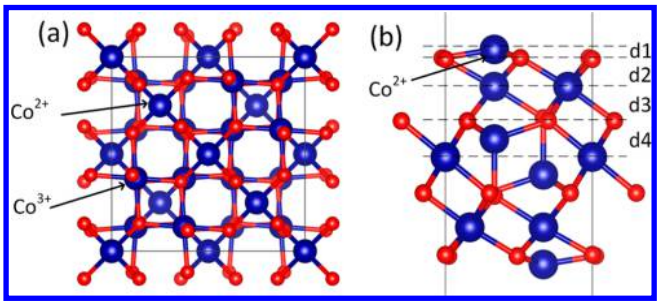


**Figure 1.** Crystal structure (a) and surface structure (b) of $Co_3O_4$ optimized using PBE-D3+U DFT, starting from the experimental crystal structure of $Co_3O_4$ (*Fd*-3*m*). Experimentally, $Co_3O_4$ is a paramagnetic semiconductor at room temperature. In this spinel structure, $Co^{2+}$ and $Co^{3+}$ are located at the interstitial tetrahedral (8a) and octahedral (16d) sites, respectively (as labeled in panel a). $Co^{2+}$ is in a $d^7$ configuration with three unpaired electrons, and $Co^{3+}$ is in a $d^6$ configuration with all of the d electrons paired. In the bulk calculation, the effective U values used 4.4 and 6.7 eV for $Co^{2+}$ and $Co^{3+}$ from literature.[16] In surface calculations, a single U value (0.59 eV) was used for all Co ions.[17] The labels in panel b are the distance of Co−O on the surface.

formula unit, which are located at the interstitial tetrahedral (8a) and octahedral (16d) sites, with 8 tetrahedral and 16 octahedral sites per cubic cell. $Co^{2+}$ is expected to have a $d^7$ high-spin configuration with three unpaired electrons, while $Co^{3+}$ is expected to have a $d^6$ configuration with all d electrons spin-paired. The PBE-D3+U DFT calculations lead to cell parameters for $Co_3O_4$ within 1% of the experimental data,[19] as shown in Table 1.

**Table 1. Comparison of the Experimental Bulk Structure[19] and Surface Structure[12] with the DFT Predicted Structures[a]**

| | bulk | (111) surface | | | |
|---|---|---|---|---|---|
| | cell parameter (a) | d1 | d2 | d3 | d4 |
| PBE+U (Å) | 8.113 | 0.29 | 0.92 | 1.04 | 0.61 |
| exp (Å) | 8.084 | 0.32 | 0.95 | 0.99 | 0.65 |

[a]Distances perpendicular to the surface (d1 to d4) are labeled in Figure 1b. All distances are in angstroms.

The surface structure predicted by DFT calculations is also consistent with experiment. We considered a symmetric slab as shown in Figure 1b. The first four Co−O distances on the surface were well reproduced by DFT calculation, as shown in Table 1. To describe the bonding of graphene to the $Co_3O_4$ (111) surface, we started with one layer of graphene distorted by 15% to match the distances of the (111) surface of $Co_3O_4$ ($5.72 \times 5.72$ Å$^2$) versus graphene ($4.92 \times 4.92$ Å$^2$), which leads to a 26% mismatch in the area. We stretched the graphene to match the $Co_3O_4$ cell parameters. Therefore, all energies are referenced to the stretched graphene. The optimized structure of one layer graphene on the oxide surface is shown in Figure 2a,c. The first contact layer is rugged, with the largest distance between rugged graphene of 2.67 Å (as shown in Figure 2c), much smaller than the interlayer distance in graphite (3.40 Å). This indicates a stronger interaction between graphene and $Co_3O_4$ than that between graphene and graphene in graphite.



DOI: 10.1021/acs.jpclett.6b02325
J. Phys. Chem. Lett. 2017, 8, 188−192

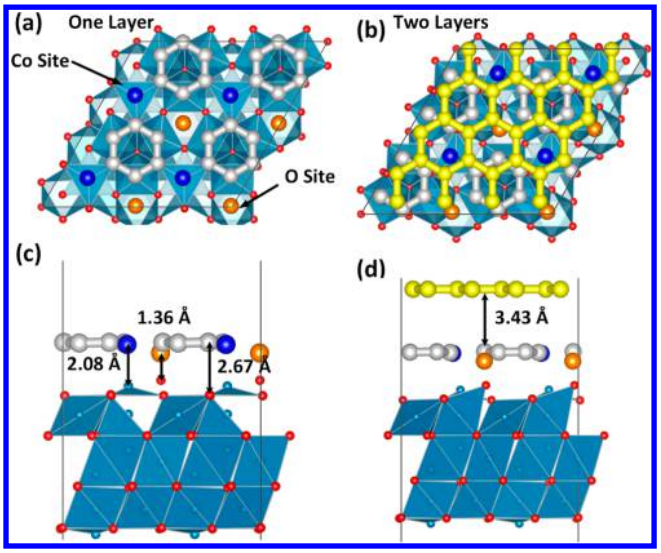


**Figure 2.** Interface structure of graphene bonded to $Co_3O_4$ (111) predicted from DFT calculation: (a,c) Top view and side view of one layer of graphene on $Co_3O_4$ and (b,d) top view and side view of two layers of graphene on $Co_3O_4$. The first contact layer of graphene is jagged due to bonding between the C of graphene with the O of the $Co_3O_4$ surface, while the second layer of graphene is very flat. The colors are Co in blue, O in red, C of the second layer in yellow, C of C6 ring in the first layer in silver, C on Co site in dark blue, and C on O site in orange.

Indeed, energy calculations show that the complex is stabilized by 0.193 eV/atom.

$$\Delta E = \frac{E^{\text{complex}} - (E^{\text{graphene}} + E^{\text{sur}})}{N_C} = -0.193 \text{ eV/atom} \quad (1)$$

The second layer of graphene was flat with mean-square displacement <0.002 Å. The distance between the first layer and the second layer of graphene is 3.42 Å, very close to the interlayer distance in graphite, which indicates that the interaction should be close to pure graphene. Indeed, we calculate a binding energy per carbon of 0.068 eV between the first ML and the stretched second ML, which is 0.015 eV stronger than between stretched graphene or unstretched graphene, 0.053 eV.

The calculations show that the first layer of graphene has a stronger interaction with $Co_3O_4$, which may be explained by the charge transfer. This −0.193 eV/atom (or −4.44 kcal/atom) energy difference is still within the range of noncovalent interactions but is much stronger than in graphite (0.05 eV/C atom). This stronger interaction may help the nucleation of graphene growth on the $Co_3O_4$ surface.

Our XPS data (Figure 3) are consistent with the calculations, indicating strong graphene-to-oxide charge transfer. C MBE at 850 K on a 10 Å thick $Co_3O_4$(111) film on Co(0001) was carried out at intervals, with annealing to 1000 K in UHV after each deposition. Prior to deposition, the Co 2p intensity (Figure 3a, solid trace) indicates $Co_3O_4$, but upon deposition of a 7.9 Å average thickness C film or ∼2.4 monolayers (ML) of graphene, the resulting spectrum (Figure 3a, open circles) shows a loss of intensity in the binding energy region of ∼779−784 eV, corresponding to reduction in the relative intensities of both $Co^{2+}$ and $Co^{3+}$ species.[20] This decrease in intensity corresponds to a decrease in average oxide thickness from 10 to 7 Å. Take-off angle-resolved Co 2p spectra (see Supporting Information, Figure S1) indicate that this oxide reduction to metal occurs near the Co oxide/Co metal interface. The amount of oxide reduced shows no further change with the formation of additional graphene layers, indicating that the cobalt oxide reduction coincides with the growth of the initial one to two graphene monolayers. The corresponding C 1s spectra (Figure 3b, solid trace) indicate that the initial C deposition yields a C 1s peak binding energy of 285.2 eV. The Co 2p and C 1s XPS spectra, therefore, indicate that initial deposition of graphene on $Co_3O_4$(111) results in charge transfer from graphene to the oxide, with partial reduction of the Co oxide to metal. This is in close agreement with the theoretical results. Deposition of additional C yields a gradual shift of the C 1s peak binding energy toward 284.5 eV (Figure 3b) upon deposition of a total of 6.4 ML graphene. The LEED pattern (Figure 3b inset), shown for the 6.4 ML film, is maintained throughout the C deposition and is the 6-fold LEED pattern characteristic of graphene. The presence of streaks rather than discrete spots indicates that the graphene sheets are azimuthally aligned. The XPS and LEED data, therefore, indicate that graphene-to-oxide charge transfer is confined to the first 1 to 2 graphene ML, again in excellent agreement with the calculations.

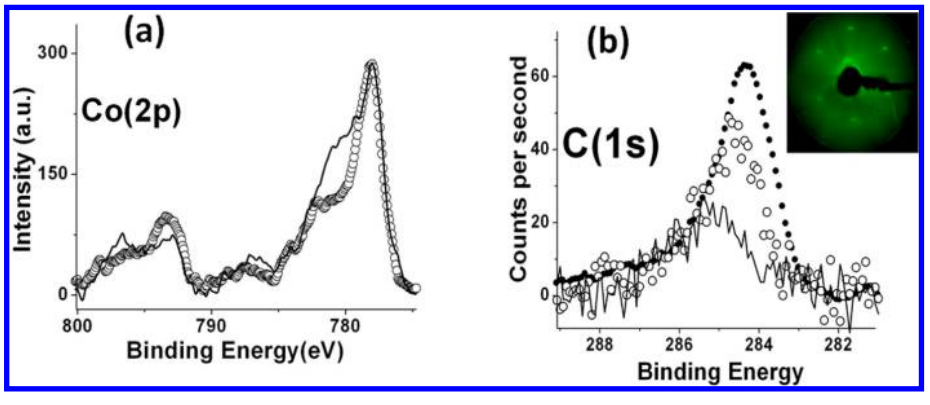


**Figure 3.** XPS spectra after C MBE on $Co_3O_4$(111): (a) XPS Co $2p_{3/2}$ spectrum before (solid trace) and after (open circles) 2.4 ML graphene deposition. The spectra have been normalized to equal maximum intensities to illustrate changes in peak shape. (b) Evolution of C 1s XPS spectra upon C deposition at 850 K and annealing to 1000 K after each deposition: (solid trace) 2.4 ML; (open circles) 5.2 ML; and (closed circles) 6.4 ML. (Inset) LEED spectrum of 6.4 ML film (150 eV beam energy).



DOI: 10.1021/acs.jpclett.6b02325
J. Phys. Chem. Lett. 2017, 8, 188−192

While it is difficult to quantify the amount of charge transfer directly from the XPS data, previously published[8] spectroscopic ellipsometry data show that graphene deposition on $Co_3O_4$ yields a 0.7 eV blue shift in the graphene $\pi \rightarrow \pi^*$ transition relative graphene on $SiO_2$ or SiC model in which the energy shift is due to interfacial dipole approximation. Assuming the sudden approximation,[21] one has

$$\Delta E = \rho\mu/\varepsilon \quad (2)$$

where $\rho$ and $\mu$ are the dipole density and magnitude and $\varepsilon$ is the (out of plane) graphene dielectric constant, taken in the low field limit.[22] The existence of such interfacial dipoles is demonstrated by Raman data showing substrate-induced enhancement of the graphene D peak intensity, the only graphene mode with an out-of-plane vibrational component.[8,9] Assuming $\Delta E \approx 0.7$ eV, equating $\rho$ with the density of C atoms in a single graphene layer, and assuming a dipole charge separation distance of ~3 Å yields an estimate of charge transfer of ~0.08 electrons/C atom in the initial graphene layer. Given the obvious uncertainties and approximations, including the number of graphene layers involved in the charge transfer, this Figure should be regarded as an estimate only, perhaps to within a factor of 2, but it is again closely consistent with the results of the DFT calculations.

We also used C-MBE to deposit a 10.5 Å form of C on $Cr_2O_3(0001)$ at 700 K. This yielded a significant C(KVV) AES feature (Figure 4a, filled circles) characteristic of $sp^2$ C[23] but no

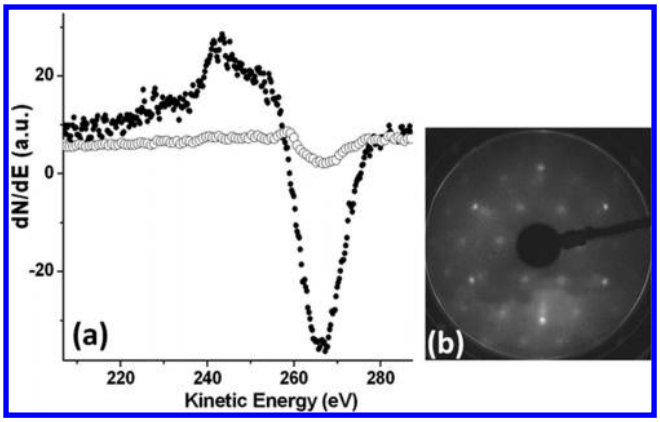


**Figure 4.** C MBE on $Cr_2O_3(0001)/Co(0001)$: (a) AES C(KVV) feature after C MBE at 700 K (filled circles) and after annealing to 850 K in UHV (open circles). (b) LEED image after C deposition at 700 K and annealing to 850 K in UHV, indicative of a vicinal $Cr_2O_3(0001)$ surface (LEED beam energy 150 eV).

observable LEED spectrum. Annealing of the disordered graphitic layer to >800 K in UHV resulted in apparent desorption of essentially all the C (Figure 4a, open circles) and a resulting LEED image (Figure 4b) characteristic of the ordered chromia/Co metal bilayer. C deposition at temperatures >800 K resulted in no significant C deposition on the chromia surface. The data in Figure 4 indicate that C MBE on $Cr_2O_3(0001)/Co(0001)$ at <800 K yields only weak C/oxide interaction, a disordered C layer, with desorption of C from the chromia surface at >800 K in UHV. This is in stark contrast with C MBE on $Co_3O_4(111)/Co(0001)$.

The weak interaction of MBE C with $Cr_2O_3(0001)$ is in direct contrast with the strong C interaction and graphene formation observed on $Co_3O_4(111)$ under nearly identical conditions. While the possible occurrence of interfacial charge transfers in the $C/Cr_2O_3(0001)$ cannot be inferred from the Auger data, previous DFT calculations on this system[6] indicate that charge transfer would flow from chromia to the graphene overlayer, the opposite of what is observed for $C/Co_3O_4(111)$. The differences in charge transfer in the graphene/$Co_3O_4$ and graphene/$Cr_2O_3$ systems cannot be ascribed to work function differences because the work functions of both oxides and graphene are all in the range of 4.5 to 4.8 eV.[24−26] We attribute differences in behavior for graphene on the two oxides to band bending in the oxide at the oxide/C interface. $Co_3O_4$ is a p-type oxide, while $Cr_2O_3$ is n-type, at least under UHV conditions.[14] The presence of positive charges in cobalt oxide surface states would enhance charge transfer from C to the oxide, whereas this would not be true for the chromia system.

In summary, theory and experiment indicate that C MBE on $Co_3O_4(111)$ results in graphene nucleation in which the partial bonding of the surface C to the substrate O atoms leads to an average charge transfer of 0.083 electrons/carbon atom from the first ML to the oxide. We find that half of the surface C form partially bonds to substrate O with an average charge transfer of +0.138 (see Figure S2) and that this charge transfer is confined to the first graphene layer. In contrast, C MBE on $Cr_2O_3(0001)$ yields only weakly interacting graphite at 700 K, with C desorption above 800 K. This is consistent with previous calculations,[6] and simple band-bending arguments indicate chromia-to-graphene charge transfer. Both theory and experiment therefore strongly suggest that the strong charge transfer from graphene to cobalt oxide is a major factor in the nucleation of graphene on this incommensurate oxide substrate during MBE. We speculate that such charge transfer is a predictive factor in graphene nucleation on other hexagonal oxide substrates.

## ■ ASSOCIATED CONTENT

### Supporting Information

The Supporting Information is available free of charge on the ACS Publications website at DOI: 10.1021/acs.jpclett.6b02325.

XPS Co(2p3/2) spectra acquired after C deposition and the distributions of charges on carbon atoms from Bader charge analysis. (PDF)

## ■ AUTHOR INFORMATION


### Corresponding Authors

*W.A.G.: E-mail: wag@wag.caltech.edu.

*J.A.K.: E-mail: Jeffry.Kelber@unt.edu; kelber@unt.edu.

### ORCID

Tao Cheng: 0000-0003-4830-177X

William A. Goddard III: 0000-0003-0097-5716


### Author Contributions

‖J.B. and T.C. contributed equally to this work.

### Notes

The authors declare no competing financial interest.

## ■ ACKNOWLEDGMENTS

Work at UNT was supported by the NSF under grant no. ECCS-1508991 and in part by C-SPIN, a funded center of STARnet, a Semiconductor Research Corporation (SRC) program sponsored by MARCO and DARPA under task IDs 2381.001 and 2381.006. The research at Caltech was supported by the NSF (DMR-1436985) and DOE (DE-SC0014607).



DOI: 10.1021/acs.jpclett.6b02325
J. Phys. Chem. Lett. 2017, 8, 188−192

## REFERENCES


(1) Tombros, N.; Jozsa, C.; Popinciuc, M.; Jonkman, H. T.; van Wees, B. J. Electronic Spin Transport and Spin Precession in Single Graphene Layers at Room Temperature. *Nature* **2007**, *448*, 571−574.

(2) Dlubak, B.; Martin, M.-B.; Deranlot, C.; Servet, B.; Xavier, S.; Mattana, R.; Sprinkle, M.; Berger, C.; De Heer, W. A.; Petroff, F.; et al. Highly Efficient Spin Transport in Epitaxial Graphene on Sic. *Nat. Phys.* **2012**, *8*, 557−561.

(3) Dlubak, B.; Seneor, P.; Anane, A.; Barraud, C.; Deranlot, C.; Deneuve, D.; Servet, B.; Mattana, R.; Petroff, F.; Fert, A. Are $Al_2O_3$ and Mgo Tunnel Barriers Suitable for Spin Injection in Graphene? *Appl. Phys. Lett.* **2010**, *97*, 092502.

(4) Haugen, H.; Huertas-Hernando, D.; Brataas, A. Spin Transport in Proximity-Induced Ferromagnetic Graphene. *Phys. Rev. B: Condens. Matter Mater. Phys.* **2008**, *77*, 115406.

(5) Stuart, S. C.; Gray, B.; Nevola, D.; Su, L.; Sachet, E.; Ulrich, M.; Dougherty, D. B. Magnetoelectric Oxide Films for Spin Manipulation in Graphene. *Phys. Status Solidi RRL* **2016**, *10*, 242−247.

(6) Choudhary, R.; Kumar, P.; Manchanda, P.; Sellmyer, D. J.; Dowben, P. A.; Kashyap, A.; Skomski, R. Interface-Induced Spin Polarization in Graphene on Chromia. *IEEE Magn. Lett.* **2016**, *7*, 1.

(7) Kelber, J. A.; Binek, C.; Bowden, P. A.; Belashchenko, K. *Magneto-Electric Voltage Controlled Spin Transistors*. U.S. Patent 9,379,232, Aug 21, 2014.

(8) Mi, Z.; Frank, L. P.; Peter, A. D.; Alex, B.; Mathias, S.; Vanya, D.; Rositza, Y.; Lingmei, K.; Jeffry, A. K. Direct Graphene Growth on $Co_3O_4$ (111) by Molecular Beam Epitaxy. *J. Phys.: Condens. Matter* **2012**, *24*, 072201.

(9) Wang, Y.; Kong, L.; Pasquale, F. L.; Cao, Y.; Dong, B.; Tanabe, I.; Binek, C.; Dowben, P. A.; Kelber, J. A.. Graphene Mediated Domain Formation in Exchange Coupled Graphene/$Co_3O_4$ (111)/Co(0001) Trilayers. *J. Phys.: Condens. Matter* **2013**, *25*, 472203.

(10) Street, M.; Echtenkamp, W.; Komesu, T.; Cao, S.; Dowben, P. A.; Binek, C. Increasing the Néel Temperature of Magnetoelectric Chromia for Voltage-Controlled Spintronics. *Appl. Phys. Lett.* **2014**, *104*, 222402.

(11) He, X.; Wang, Y.; Wu, N.; Caruso, A. N.; Vescovo, E.; Belashchenko, K. D.; Dowben, P. A.; Binek, C. Robust Isothermal Electric Control of Exchange Bias at Room Temperature. *Nat. Mater.* **2010**, *9*, 579−585.

(12) Meyer, W.; Biedermann, K.; Gubo, M.; Hammer, L.; Heinz, K. Surface Structure of Polar $Co_3O_4$ (111) Films Grown Epitaxially on Ir(100)-(1 × 1). *J. Phys.: Condens. Matter* **2008**, *20*, 265011.

(13) Xiao, W.; Xie, K.; Guo, Q.; Wang, E. G. Growth and Electronic Structure of Cu on $Cr_2O_3$ (0001). *J. Phys.: Condens. Matter* **2003**, *15*, 1155.

(14) Kofstad, P.; Lillerud, K. P. On High Temperature Oxidation of Chromium: Ii. Properties of and the Oxidation Mechanism of Chromium. *J. Electrochem. Soc.* **1980**, *127*, 2410−2419.

(15) Beatty, J.; Cao, Y.; Tanabe, I.; Sky Driver, M.; Dowben, P. A.; Kelber, J. A. Atomic Layer-by-Layer Deposition of H-Bn(0001) on Cobalt: A Building Block for Spintronics and Graphene Electronics. *Mater. Res. Express* **2014**, *1*, 046410.

(16) Chen, J.; Wu, X.; Selloni, A. Electronic Structure and Bonding Properties of Cobalt Oxide in the Spinel Structure. *Phys. Rev. B: Condens. Matter Mater. Phys.* **2011**, *83*, 245204.

(17) Chen, J.; Selloni, A. Electronic States and Magnetic Structure at the $Co_3O_4$ (110) Surface: A First-Principles Study. *Phys. Rev. B: Condens. Matter Mater. Phys.* **2012**, *85*, 085306.

(18) Chen, H.; Kolpak, A. M.; Ismail-Beigi, S. Electronic and Magnetic Properties of $SrTiO_3/LaAlO_3$ Interfaces from First Principles. *Adv. Mater.* **2010**, *22*, 2881−2899.

(19) Smith, W. L.; Hobson, A. D. The Structure of Cobalt Oxide, $Co_3O_4$. *Acta Crystallogr., Sect. B: Struct. Crystallogr. Cryst. Chem.* **1973**, *29*, 362−363.

(20) Petitto, S. C.; Langell, M. A. Surface Composition and Structure of $Co_3O_4$(110) and the Effect of Impurity Segregation. *J. Vac. Sci. Technol., A* **2004**, *22*, 1690−1696.

(21) Foster, K. W.; Saranak, J.; Dowben, P. A. Spectral Sensitivity, Structure and Activation of Eukaryotic Rhodopsins: Activation Spectroscopy of Rhodopsin Analogs in Chlamydomonas. *J. Photochem. Photobiol., B* **1991**, *8*, 385−408.

(22) Santos, E. J. G.; Kaxiras, E. Electric-Field Dependence of the Effective Dielectric Constant in Graphene. *Nano Lett.* **2013**, *13*, 898−902.

(23) Viljoen, P. E.; Roos, W. D.; Swart, H. C.; Holloway, P. H. Carbon Auger Peak Shape Measurements in the Characterization of Reactions on (001) Diamond. *Appl. Surf. Sci.* **1996**, *100*, 612−616.

(24) Yu, T.; Zhu, Y. W.; Xu, X. J.; Shen, Z. X.; Chen, P.; Lim, C. T.; Thong, J. T. L.; Sow, C. H. Controlled Growth and Field-Emission Properties of Cobalt Oxide Nanowalls. *Adv. Mater.* **2005**, *17*, 1595−1599.

(25) Wilde, M.; Beauport, I.; Stuhl, F.; Al-Shamery, K.; Freund, H. J. Adsorption of Potassium on $Cr_2O_3$(0001) at Ionic and Metallic Coverages and Uv-Laser-Induced Desorption. *Phys. Rev. B: Condens. Matter Mater. Phys.* **1999**, *59*, 13401−13412.

(26) Yu, Y.-J.; Zhao, Y.; Ryu, S.; Brus, L. E.; Kim, K. S.; Kim, P. Tuning the Graphene Work Function by Electric Field Effect. *Nano Lett.* **2009**, *9*, 3430−3434.




DOI: 10.1021/acs.jpclett.6b02325
*J. Phys. Chem. Lett.* 2017, 8, 188−192